Princeton Plasma Physics Laboratory

PPPL-4074

PPPL-4074

Measurement of Turbulence Decorrelation during Transport Barrier Evolution in a High Temperature Fusion Plasma

R. Nazikian, K. Shinohara, G.J. Kramer, E. Valeo, K. Hill,
T.S. Hahm, G. Rewoldt, S. Ide, Y. Koide,
Y. Oyama, H. Shirai, and W. Tang

May 2005

Prepared for the U.S. Department of Energy under Contract DE-AC02-76CH03073.

Measurement of Turbulence Decorrelation during Transport Barrier Evolution in a High Temperature Fusion Plasma

R. Nazikian[1], K. Shinohara[2], G.J. Kramer[1], E. Valeo[1], K. Hill[1], T.S. Hahm[1], G. Rewoldt[1], S. Ide[2], Y. Koide[2], Y. Oyama[2], H. Shirai[2], W. Tang[1]

[1]Princeton Plasma Physics Laboratory, P.O. Box 451, Princeton NJ 08540, USA

[2]Japan Atomic Energy Research Institute, Naka Fusion Research Establishment 311-0193, Muko-yama 801-1, Naka-machi, Naka-gun, Ibaraki, Japan

Abstract

A low power polychromatic beam of microwaves is used to diagnose the behavior of turbulent fluctuations in the core of the JT-60U tokamak during the evolution of the internal transport barrier. A continuous reduction in the size of turbulent structures is observed concomitant with the reduction of the density scale length during the evolution of the internal transport barrier. The density correlation length decreases to the order of the ion gyroradius, in contrast to the much longer scale lengths observed earlier in the discharge, while the density fluctuation level remain similar to the level before transport barrier formation.

A milestone in the understanding and control of turbulent transport was the discovery of the High confinement regime (H-mode) in the ASDEX device [1]. The H-mode is characterized by a sudden reduction of thermal diffusion in a thin layer known as a transport barrier near the periphery of the toroidal plasma column. The formation of the transport barrier is correlated with a reduction in the turbulent fluctuations and turbulence induced transport. More recently, further improvement in the stored energy of magnetic confinement systems has been achieved through the spontaneous development of internal transport barriers [2]. Unlike the plasma edge, much less is known about core transport barriers, principally due to the difficulty of turbulence measurements in the central region of the discharge. The specific mechanism for the activation and evolution of core transport barriers is still poorly understood, although indirect evidence suggests a key role played by ExB velocity shear, Shafranov shift and reversed magnetic shear [3-7] in suppressing turbulence induced transport.

One method with the potential to probe turbulent fluctuations in the plasma core is correlation reflectometry, where multiple microwave beams are launched into the plasma and reflected from density irregularities at different plasma radii [8. 9]. The diagnostic method (analogous to Ionosonde in ionospheric research [10]) uses the pattern of waves reflected from turbulence near a cutoff layer to extract information on the structure of the turbulent eddies. In this paper we report on the direct measurement of the radial correlation length of core turbulence during the evolution of the internal transport barrier in the JT-60U tokamak [11, 12] using the method of reflectometry. The measurements employ the simultaneous reflection of multiple microwave beams from the plasma core, together with full wave simulations [13-15] in the real plasma geometry in order to infer the scale length and magnitude of density fluctuations during transport barrier evolution.

Microwaves in the frequency range 115-140 GHz are launched into the JT-60U device along the toroidal plasma midplane. The microwaves are launched in the X-mode (microwave electric field polarized perpendicular to the plasma magnetic field) so that the reflecting layer is determined by a combination of the magnetic field strength and the plasma density [16]. The full wave simulation of the scattered electric field intensity in the real JT-60U plasma geometry is illustrated in Fig. 1a. The waves scatter from density irregularities near the reflecting layer and returns to the launching antenna, establishing a standing wave pattern in the electric field. Figure 1b is a magnified view of the reflecting region showing the standing wave pattern of incoming and outgoing waves in the presence of density fluctuations. The density fluctuations are generated using an ad hoc model based on a random distribution satisfying a given two-point correlation function with a predetermined poloidal and radial scale length and fluctuation magnitude [13, 15].

The JT-60U device has achieved the highest equivalent fusion power performance to date through the use of internal transport barriers that expand out to large radii in the plasma column. Internal transport barriers tend to form in discharges where the plasma current profile is broadened or peaked away from the plasma center (or magnetic axis). The broadening of the current profile can be achieved by increasing the inductance of the core plasma through early preheat using neutral beam injection, and by ramping the plasma current up rapidly [11]. Such discharges exhibit spontaneous transitions to states of enhanced core confinement.

Figure 2 shows an example of a discharge exhibiting a transition to enhanced core confinement. The bifurcation in the energy transport is seen as a sudden increase of the core ion temperature during high power neutral beam injection starting at 5.05 s. The transition is followed by the evolution of very flat density and temperature profiles in the central region of the discharge, together with a very steep pressure gradient separating the core from the outer region of the plasma. The trajectory of the reflecting layer for a 115 GHz microwave beam propagating along the plasma midplane is indicated by the intersection of the red arrow in Fig. 2c with the density profiles shown at different times.

At the start of high power neutral beam injection the reflecting positions of the microwaves occur in the range 0 - 0.25 m from the plasma center for the discharge shown in Fig. 2. Figure 3 displays the evolution of the radial correlation length of reflected waves from the plasma core at different times and at different radii following high power neutral beam injection. The spectrum of reflected waves is shown in Fig 3a. The symmetry of the spectrum indicates very good alignment of the incident and reflected waves to the reflecting surface. These discharges were also carefully chosen to be free of any contamination on the reflected signal from MHD activity. Figure 3b shows a continuous reduction of the radial correlation length of the reflected waves from just after high power neutral beam injection through to the fully formed transport barrier. Figure 3c shows a strong (linear) correlation between the radial correlation length obtained from the raw reflectometer data and the density scale length inside the steep pressure gradient region of the internal transport barrier. The data indicates that the reduction in the radial correlation length is concomitant with the reduction of the pressure scale length inside the transport barrier. Also note that the ion temperature is approximately constant along the trajectory of the reflecting layer in this discharge.

The initial radial decorrelation of the turbulent fluctuations (between t=5.10 s to 5.35 s in Fig. 3b) takes place well before the observation of steep pressure gradients in the fully formed transport barrier. The initial decorrelation starts almost immediately after high power neutral beam injection at 5.05 s. One remarkable feature of this data is the very long radial scale lengths (> 20 cm) observed in the fluctuations before and immediately after high power neutral beam injection.

For the quantitative interpretation of the fluctuation magnitude and radial correlation length we use a full wave code that has been validated through detailed benchmarking to Langmuir probe measurements in laboratory plasmas [13, 15]. The full wave analysis is performed at two times in the evolution of the discharge, the first just before the injection of high neutral beam power and the second at the time of the fully formed transport barrier (corresponding to the curve at 6.12 s in Fig 3b). Figure 4a shows experimental correlation data (red squares) together with simulation results for data taken before the start of high power neutral beam injection. The measured correlation length before high power beam injection extends across the entire central region of the plasma, so that the correlation length is of the order of the local minor radius. From 1-D and 2-D full wave simulations, the measurements are consistent with a radial correlation length $\lambda_r \approx 20$ cm and a density fluctuation level $\delta n/n \approx 5x10^{-4}$ within ±10 cm of the magnetic axis. An important result from the 2-D full wave simulations is that the inferred radial correlation length and local fluctuation level are only weakly dependent on the degree of anisotropy (poloidal wavelength) of the model fluctuations. For a central ion temperature of 5 keV this gives an inferred radial fluctuation scale length of $k_r\rho_i \approx 0.03$ (where ρ_i is the thermal ion gyroradius and $k_r = 2/\lambda_r$ for a Gaussian radial correlation function). The radial scale length for these broadband fluctuations is much greater than the typical scale length ($k_r\rho_i \approx 0.1$-0.5) expected for Ion Temperature Gradient (ITG) driven turbulence.

In contrast, Figure 4b shows the correlation data obtained in the steep pressure gradient region of the fully formed internal transport barrier at 6.12 s in discharge E32844. The best fit to the data from 1-D and 2-D simulations is obtained for a radial density correlation length of approximately 4 mm and a local fluctuation level of ≈0.5%. Note that the fluctuation level is approximately a factor of two higher than measured at a similar minor radius on the high field side of the magnetic axis immediately before high power neutral beam injection.

Modeling analysis reveals that the measurement is actually very close to the resolution limit of the diagnostic as indicated by the innermost curve corresponding to $\lambda_r = 2.5$ mm (dashed line in Fig. 4b). Thus, we do not preclude the possibility that the actual radial correlation length of turbulence in the transport barrier may be shorter than 4 mm. The radial scale length of 4 mm corresponds to $k_r\rho_i \approx 1$ for an ion temperature of 5 keV in the center of the transport barrier. The scale length is barely two ion gyroradii or less, suggesting that the dominant drive for these fluctuations is not coming from the ion temperature gradient but from the trapped electron population for drift type modes. [17]

Figure 5 shows the radial profile of the inferred density fluctuation level from microwave reflectometer measurements together with the calculated linear growth rate for drift wave type modes obtained using the FULL local microinstability code [17]. Analysis is shown at two times in the discharge for Fig. 5a and Fig. 5b corresponding to the timing of Fig 4a and Fig 4b respectively. Note that the absolute level of density fluctuations is relatively similar at the two times at the radius (r=±0.3 m) corresponding to the position of the internal transport barrier. Two linear growth rate profiles from the FULL code are displayed below the reflectometer data, one with and the other without the effect of ExB shear. A key result from the linear stability analysis is that the growth rate is not fully suppressed by the ExB velocity shear however the location, width and strength of the instability drive is affected by the presence of ExB shear.

An important observation is the apparent similarity of the density fluctuation level in the target and fully developed internal transport barrier plasmas at the minor radius $r \approx \pm 30$ cm. Suppression of the fluctuation level has been seen in other experiments at the transition to enhanced core confinement; however fluctuation levels have also been seen to increase after the transition [18, 19]. For this reason, the relation between fluctuation suppression and barrier formation is still not entirely clear. For simplicity, let us suppose that the fluctuation magnitude can be related to the radial correlation length using the mixing length assumption $\delta n/n \approx \lambda_r/L_M$ in the strong turbulence regime [20] and $\delta n/n \approx (\gamma_{lin}/\Delta\omega)^{1/2}(\lambda_r/L_M)$ in the weak turbulence regime [21]. Here, L_M is a macroscopic scale length (typically a combination of the density and temperature scale lengths) and λ_r is the fluctuation radial correlation length. In both the strong and weak turbulence regimes, the reduction in the radial correlation length could occur without much reduction in the fluctuation magnitude so long as the density gradient scale length is simultaneously decreasing. Note that the ratio of the radial correlation length to the density scale length is approximately constant inside the transport barrier (see Fig. 3c) so that the weak variation of the fluctuation level is consistent with mixing length arguments. Indeed, for a radial correlation length of 4mm (Fig. 4b) and a density scale length of 10 cm (Fig. 3c at 6.12 s), then the observed density fluctuation level of 0.5% is in good quantitative agreement with mixing length estimates in the strong turbulence regime.

It is interesting that a finite fluctuation level is also observed in edge transport barriers (H-mode plasmas) at or near the pre-barrier fluctuation level with short scale features of the order of the ion poloidal gyro-radius [7]. Note that the Ion Temperature Gradient (ITG) drive is predicted to be weak compared to the Trapped Electron (TE) drive for the short scale features observed in the steep pressure gradient region of the internal transport barrier in JT-60U. The effect of a transition from ITG drive at large scales to TE drive at short scale needs further investigation.

The large reduction in the turbulent correlation length may indicate a concomitant reduction in the anomalous diffusivity inside the JT-60U transport barrier. A large reduction in the thermal and particle diffusivity has indeed been inferred in similar discharges from power balance considerations [11]. Note however that a diffusion coefficient can decrease without a net decrease in the radial anomalous flux so long as the plasma gradients increase on the same time scale. Therefore, we cannot make a definitive statement regarding transport flux reduction from the available data. A more definitive conclusion on flux reduction will require the direct measurement of key plasma quantities that appear in the expression of the anomalous radial flux such as the potential fluctuations, poloidal wave number spectra, as well as the cross phase between potential and density fluctuations. Obtaining direct measurements of these quantities presents a grand challenge to experimental fusion science.

An interesting observation in the data is that the radial correlation length before transport barrier formation is of the order of the local minor radius (≈20 cm) before injection of high power neutral beams, which suggests that a purely local description of turbulence is quite inadequate in these regions. Also the scale length greatly exceeds the range expected for drift type modes. This may indicate that the broadband feature in the plasma core is something other than drift waves, but so far there is no model known to the authors that can account for such large-scale features. Another non-local effect may be occurring inside the steep pressure gradient region of the fully formed transport barrier. From Figure 5b, it is apparent that the growth rate from the FULL code analysis with ExB shear peaks at the foot of the transport barrier and is negative in regions where fluctuation are observed with the reflectometer. This suggests that a process of turbulence spreading may be occurring from linearly unstable to linearly stable regions inside the transport barrier [22].

Much work still needs to be done in order to construct a detailed picture of transport barrier dynamics in fusion plasmas. On the experimental side many more microwave beams are needed than are currently employed in any existing experiment to fully characterize the evolution of fluctuations across the core plasma profile. On the computational side, careful linear analysis of threshold conditions for the onset of turbulent phenomena reveal a great deal about the underlying instabilities; however many key questions demand a proper nonlinear treatment.

Acknowledgements

Thanks go to R. Yoshino and H. Ninomia at JAERI and to K. Young and N. Sauthoff at PPPL for initiating this collaborative program. This work is supported by DOE Contract # DE-AC02-76-CH03073 and by the Japan Atomic Energy Research Institute and is implemented under the International Energy Agency's co-operation agreement on Large Tokamak Facilities established between JAERI, DOE and EURATOM.

References

[1] F. Wagner et al., PRL **49**, 1408 (1982)

[2] Y. Koide, M. Kikuchi et al., Phys. Rev. Lett., **72** 3662 (1994).

[3] H. Biglari, P.H. Diamond, and P.W. Terry, Phys. Fluids B **2**, 1 (1990).

[4] T.S. Hahm and K.H. Burrell, Phys. Plasmas **2**, 1648 (1995)

[5] K. H. Burrell, Phys. Plasmas **4**, 1499 (1997)

[6] E.J. Synakowski, S.H. Batha, M.A. Beer *et al.*, Phys. Rev. Lett. **78**, 2972 (1997)

[7] E.J. Synakowski et al., Plasma Physics and Controlled Fusion **44** A165-A173 (2002)

[8] P. Cripwell, A.E. Costley and A.E. Hubbard, *Proceedings, 16th European Physical Society Conference on Plasma Physics and Controlled Fusion, Venice, 1989,* (EPS, 1989) Vol. **1**, p. 75.

[9] A.E. Costley, P. Cripwell, R. Prentice and A.C.C. Sips, Rev. Sci. Inst. **61**, 2823 (1990).

[10] J.A. Ratcliffe, Nature, **No. 4105**, p.9 (1948)

[11] T. Fujita et al., PRL **78**, 2377 (1997)

[12] K. Shinohara, et al., Rev. Sci. Instrum., **70**, 4246 (1999)

[13] E. Valeo, G.J. Kramer, and R. Nazikian, *Plasma Phys. Control. Fusion* **44** L1 (2002)

[14] M. Gilmore, W.A. Peebles and X.V. Nguyen, Plasma Phys. Control. Fusion **42**, L1 (2000).

[15] G.J. Kramer et al., Rev. Sci. Instrum., **74**, 1421 (2003).

[16] E. Mazzucato and R. Nazikian, Phys. Rev. Lett. **71**, 1840 (1993)

[17] G. Rewoldt, et al., Nuclear Fusion, **42,** 403 (2002).

[18] E. Mazzucato, S.H. Batha, M. Beer *et al.*, Phys. Rev. Lett **77**, 3145 (1996).

[19] G.D. Conway, D.N. Borba, B. Alper *et al.*, Phys. Rev. Lett., **84**, 1463 (2000).

[20] W. Horton, Rev. Mod. Phys. **71**, 735 (1999).

[21] R.Z. Sagdeev and A.A. Galeev, in Nonlinear Plasma Theory, edited by T.M. O'Neil and D.L. Book (Benjamin, New York, 1969).

[22] T. S. Hahm et al., Plasma Physics and Controlled Fusion **46**, A323 (2004)

Figures Captions

Figure 1

Full wave simulation of the intensity of launched and reflected microwaves from an initial Gaussian profile beam at 115 GHz in a JT-60U plasma (a). Density fluctuations of 0.5% are imposed on the plasma reflecting layer. An enlargement of the reflecting region is shown in (b). Corrugations in the fringe pattern of incoming and outgoing waves are induced by the imposed density fluctuations at the cutoff layer.

Figure 2

The evolution of plasma parameters during the formation of the internal transport barrier in JT-60U with (a) the evolution of the plasma current and neutral beam heating power; (b) the central ion temperature at two radii; and (c) the buildup of the core plasma density during the evolution of the transport barrier. The red arrow in (c) corresponds to the trajectory of the X-mode reflecting layer at 115 GHz throughout the discharge. The discharge parameters are: Toroidal field 3.5 T, plasma current 1.3 MA, major radius 3.2 m, minor radius 0.96 m.

Figure 3

(a) Spectrum of reflected waves just after high power beam injection; (b) reflectometer correlation vs. radial separation of reflecting layers at different times through the discharge; and (c) radial correlation length of reflectometer signals vs. the density scale length in the transport barrier from 5.82 s to 6.12 s. Each data point corresponds to a 120 ms integration time. The ion temperature stays near 5 keV ($\rho_I \approx 2.5$ mm) along the trajectory of the reflecting position for all these times. Note that the ratio of the reflectometer correlation length to the density scale length is roughly constant during the build up of the transport barrier from 5.82 s to 6.12 s (see red arrow in Fig. 2 for trajectory of reflecting layer).

Figure 4

Radial correlation data together with full wave simulations at two times, before high power neutral beam heating in (a) and in the fully developed internal transport barrier in (b). The measured correlations (red squares) are compared to 1-D (solid line) and 2-D full wave simulations (diamonds). In (a) a density correlation length $\lambda_r \approx 20$ cm is inferred consistent with the 1-D and 2-D modeling. The 2-D modeling shows that the estimated correlation length is only weakly dependent on the choice of the poloidal (vertical) scale length. In (b) data are shown in red squares, and 1-D modeling results are shown for k_r=5 cm^{-1} (solid line) and 8 cm^{-1} (dashed line). 2-D full wave simulations (diamond) are shown for k_r = 5 cm^{-1} and for a range of poloidal scales (k_θ=0, 2, 5 cm^{-1}) indicating the robustness of the inferred radial scale length to large variations in the poloidal scale length. The data and 2-D model analysis exhibit a statistical spread indicated by the inset error bar.

Figure 5

Inferred density fluctuation level (blue) and the plasma density profile (red) in the target plasma (a) and in the internal transport barrier plasma (b) compared to the calculated linear growth rate (bottom) using the FULL code without rotation (purple) and with rotation (green). The calculated linear growth rate is only plotted in the region where there are reflectometer measurements. The yellow shaded regions indicate the radial extent of linearly unstable modes calculated with rotation.

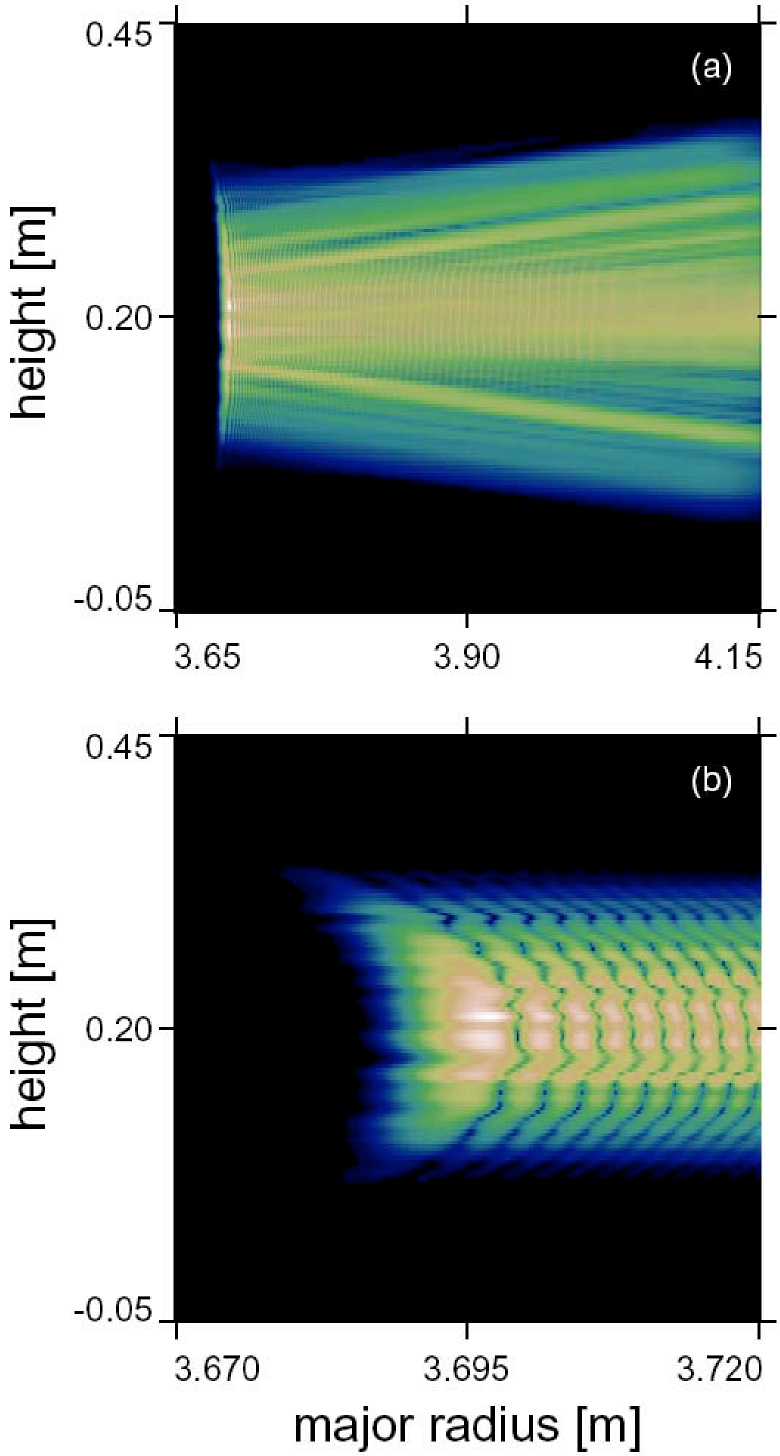
0.45
0.20
-0.05
height [m]
(a)
3.65
3.90
4.15
0.45
0.20
-0.05
height [m]
(b)
3.670
3.695
3.720
major radius [m]

Fig. 1

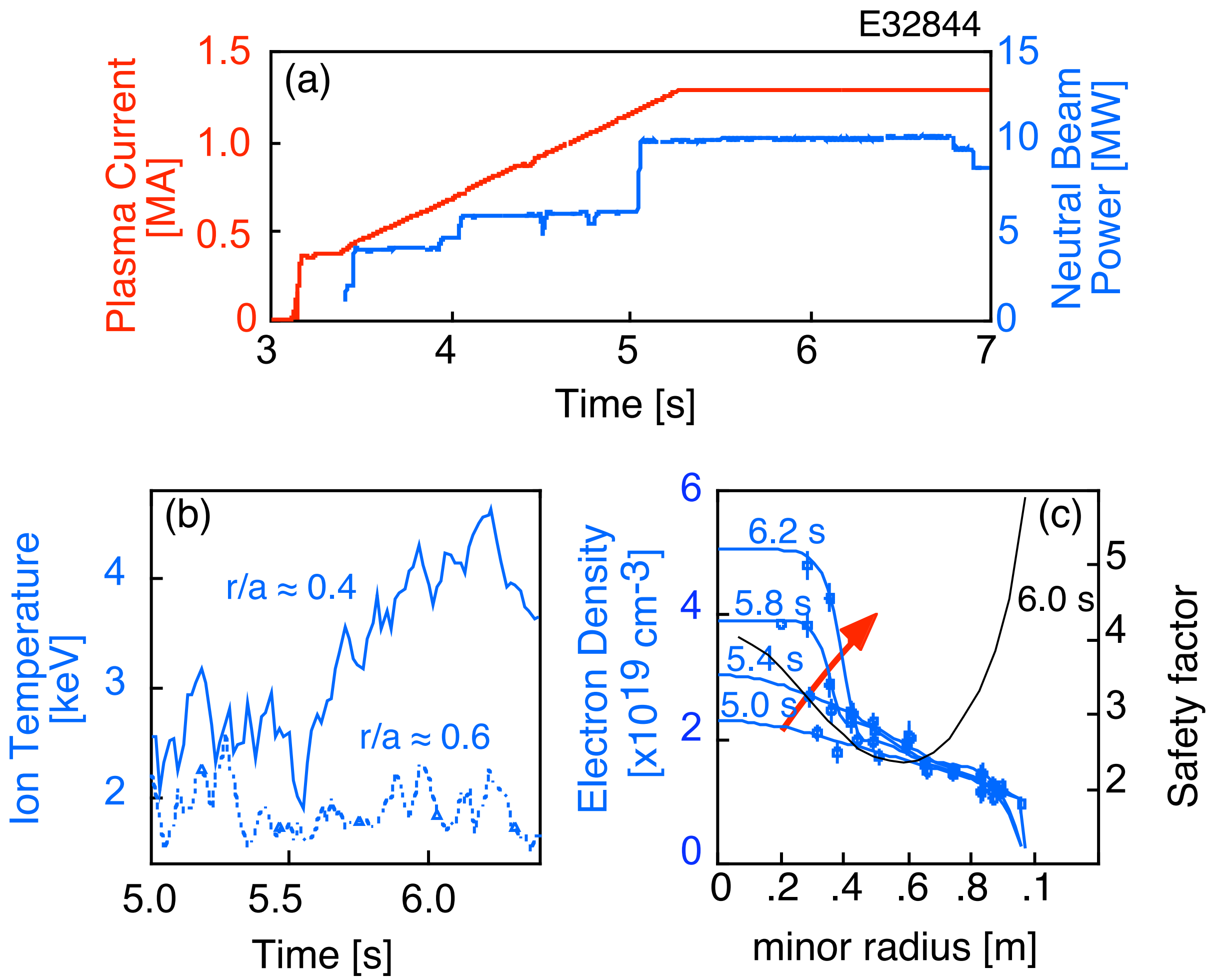

E32844
(a)
Plasma Current [MA]
1.5
1.0
0.5
0
Neutral Beam Power [MW]
15
10
5
0
3
4
5
6
7
Time [s]
(b)
Ion Temperature [keV]
4
3
2
r/a ≈ 0.4
r/a ≈ 0.6
5.0
5.5
6.0
Time [s]
(c)
Electron Density [x1019 cm-3]
6
4
2
0
6.2 s
5.8 s
5.4 s
5.0 s
6.0 s
Safety factor
5
4
3
2
0
.2
.4
.6
.8
.1
minor radius [m]

Fig. 2

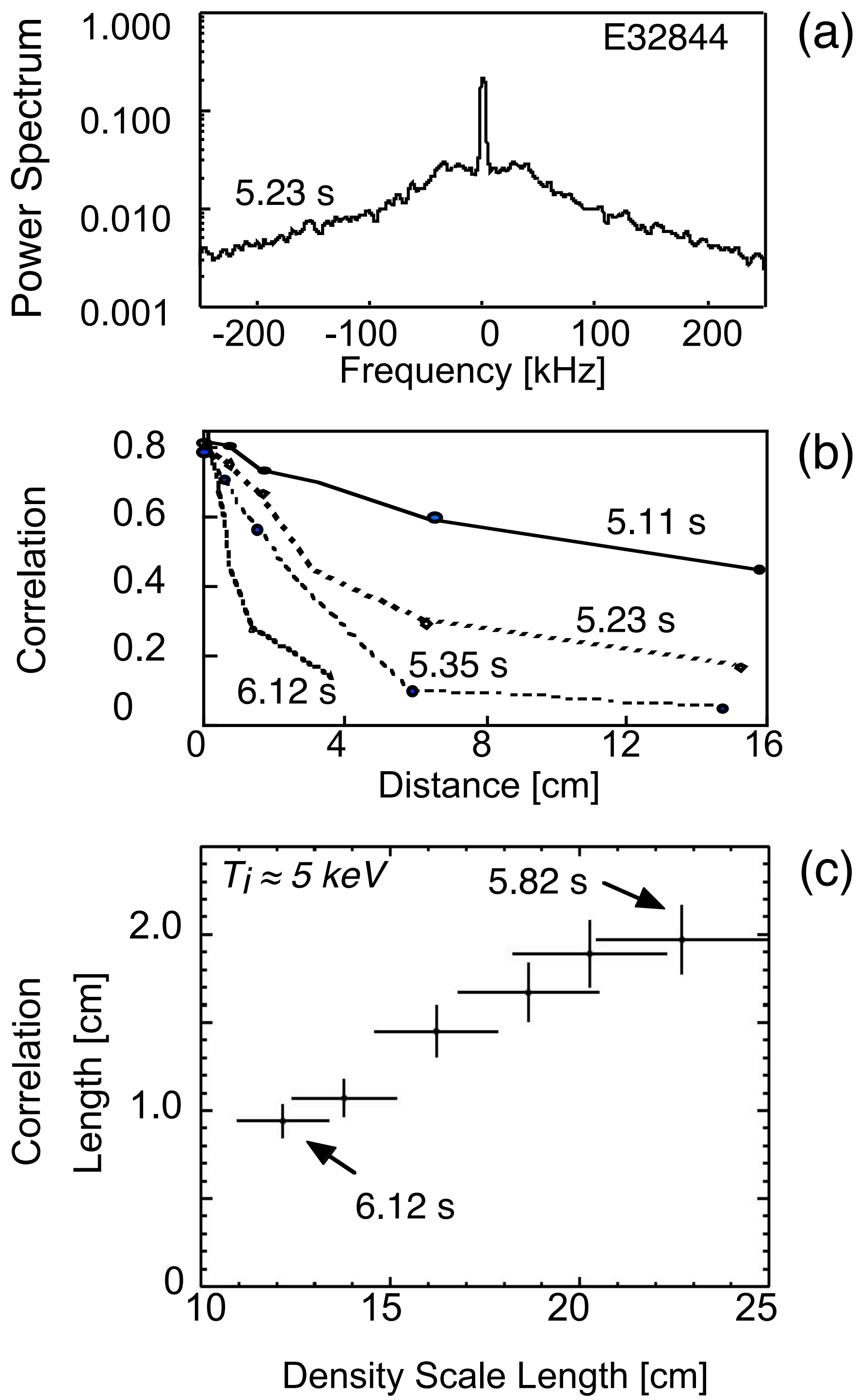

(a)
E32844
Power Spectrum
1.000
0.100
0.010
0.001
5.23 s
-200
-100
0
100
200
Frequency [kHz]
(b)
Correlation
0.8
0.6
0.4
0.2
0
5.11 s
5.23 s
5.35 s
6.12 s
0
4
8
12
16
Distance [cm]
(c)
$T_i \approx 5$ keV
5.82 s
Correlation Length [cm]
2.0
1.0
0
6.12 s
10
15
20
25
Density Scale Length [cm]

Fig. 3

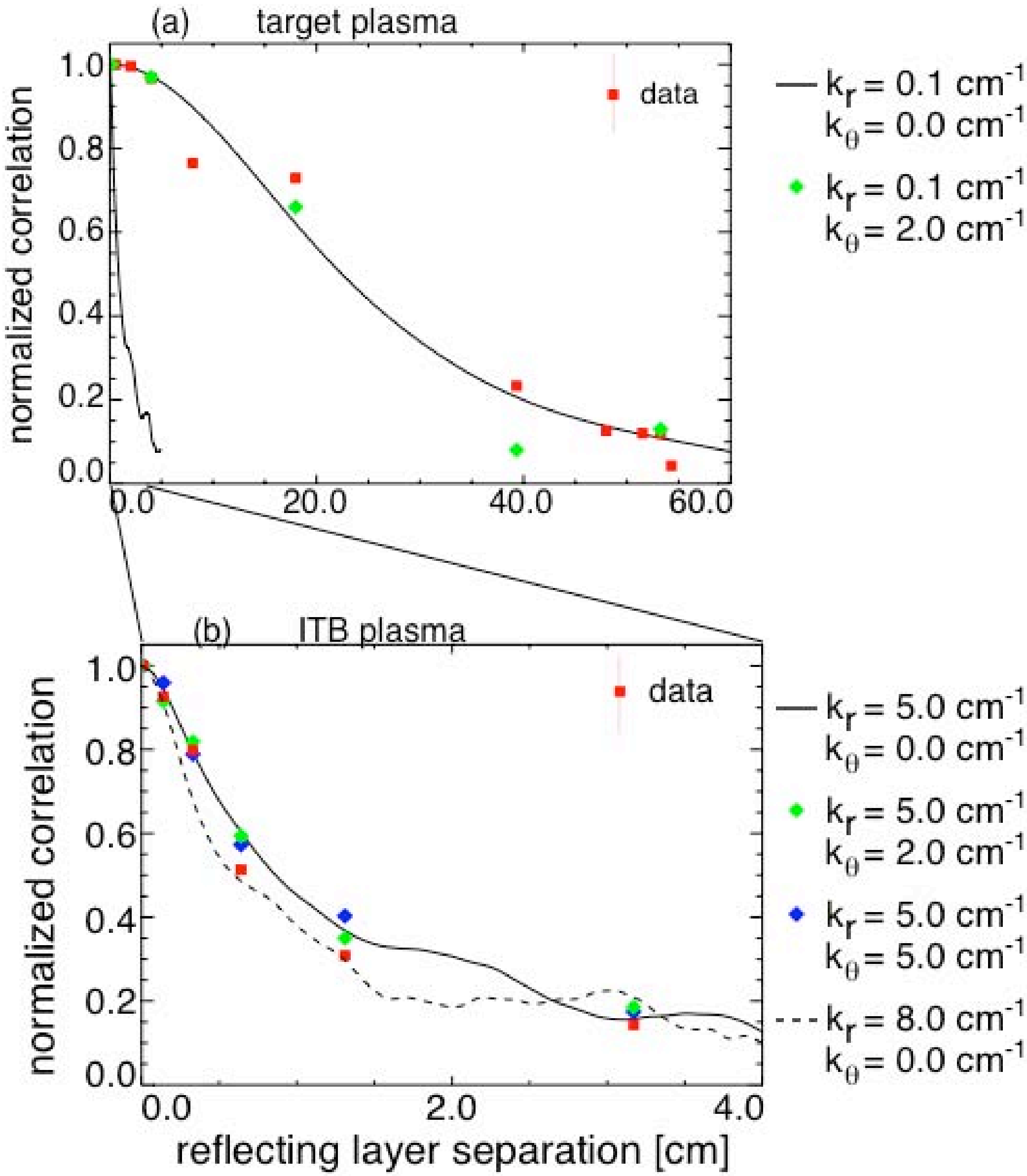
(a) target plasma
normalized correlation
1.0
0.8
0.6
0.4
0.2
0.0
0.0
20.0
40.0
60.0
data
kr = 0.1 cm-1
kθ = 0.0 cm-1
kr = 0.1 cm-1
kθ = 2.0 cm-1
(b) ITB plasma
normalized correlation
1.0
0.8
0.6
0.4
0.2
0.0
0.0
2.0
4.0
reflecting layer separation [cm]
data
kr = 5.0 cm-1
kθ = 0.0 cm-1
kr = 5.0 cm-1
kθ = 2.0 cm-1
kr = 5.0 cm-1
kθ = 5.0 cm-1
kr = 8.0 cm-1
kθ = 0.0 cm-1

Fig. 4

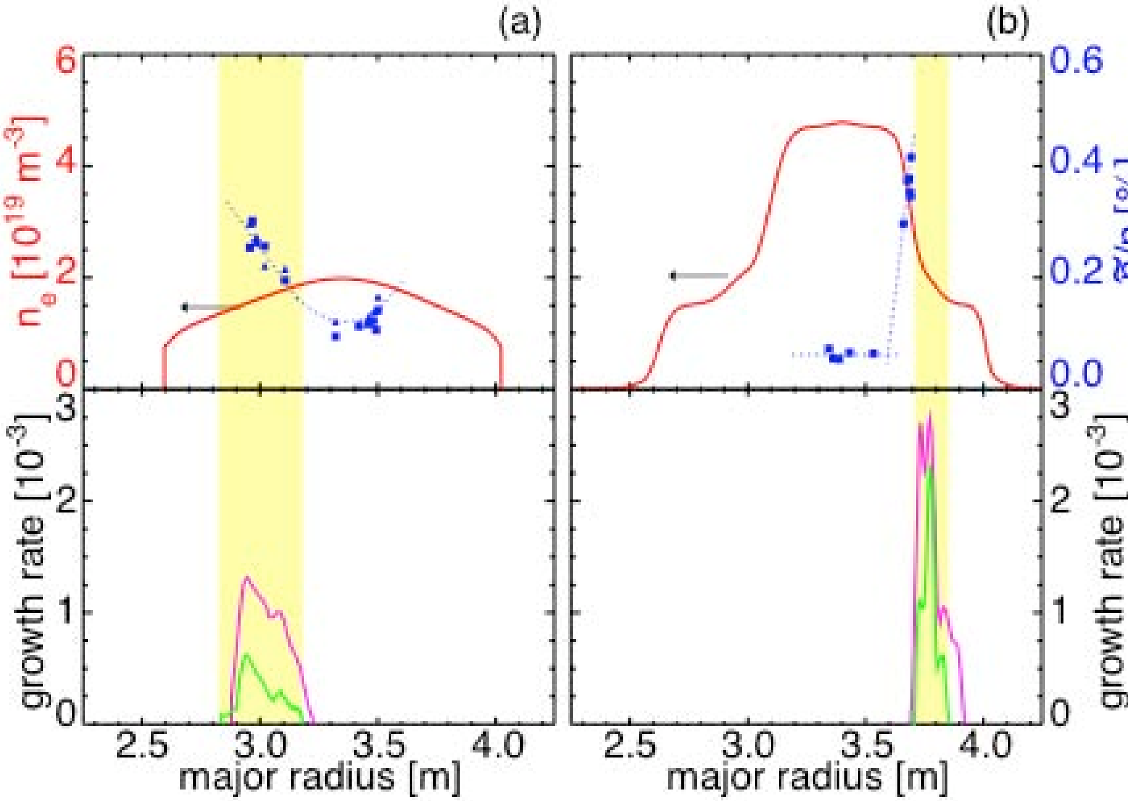

(a)
(b)
n_e [10^{19} m^{-3}]
$\tilde{n}/n$ [%]
growth rate [10^{-3}]
growth rate [10^{-3}]
major radius [m]
major radius [m]

Fig. 5

External Distribution

Plasma Research Laboratory, Australian National University, Australia
Professor I.R. Jones, Flinders University, Australia
Professor João Canalle, Instituto de Fisica DEQ/IF - UERJ, Brazil
Mr. Gerson O. Ludwig, Instituto Nacional de Pesquisas, Brazil
Dr. P.H. Sakanaka, Instituto Fisica, Brazil
The Librarian, Culham Science Center, England
Mrs. S.A. Hutchinson, JET Library, England
Professor M.N. Bussac, Ecole Polytechnique, France
Librarian, Max-Planck-Institut für Plasmaphysik, Germany
Jolan Moldvai, Reports Library, Hungarian Academy of Sciences, Central Research Institute for Physics, Hungary
Dr. P. Kaw, Institute for Plasma Research, India
Ms. P.J. Pathak, Librarian, Institute for Plasma Research, India
Dr. Pandji Triadyaksa, Fakultas MIPA Universitas Diponegoro, Indonesia
Professor Sami Cuperman, Plasma Physics Group, Tel Aviv University, Israel
Ms. Clelia De Palo, Associazione EURATOM-ENEA, Italy
Dr. G. Grosso, Instituto di Fisica del Plasma, Italy
Librarian, Naka Fusion Research Establishment, JAERI, Japan
Library, Laboratory for Complex Energy Processes, Institute for Advanced Study, Kyoto University, Japan
Research Information Center, National Institute for Fusion Science, Japan
Professor Toshitaka Idehara, Director, Research Center for Development of Far-Infrared Region, Fukui University, Japan
Dr. O. Mitarai, Kyushu Tokai University, Japan
Mr. Adefila Olumide, Ilorin, Kwara State, Nigeria
Dr. Jiangang Li, Institute of Plasma Physics, Chinese Academy of Sciences, People's Republic of China
Professor Yuping Huo, School of Physical Science and Technology, People's Republic of China
Library, Academia Sinica, Institute of Plasma Physics, People's Republic of China
Librarian, Institute of Physics, Chinese Academy of Sciences, People's Republic of China
Dr. S. Mirnov, TRINITI, Troitsk, Russian Federation, Russia
Dr. V.S. Strelkov, Kurchatov Institute, Russian Federation, Russia
Kazi Firoz, UPJS, Kosice, Slovakia
Professor Peter Lukac, Katedra Fyziky Plazmy MFF UK, Mlynska dolina F-2, Komenskeho Univerzita, SK-842 15 Bratislava, Slovakia
Dr. G.S. Lee, Korea Basic Science Institute, South Korea
Dr. Rasulkhozha S. Sharafiddinov, Theoretical Physics Division, Insitute of Nuclear Physics, Uzbekistan
Institute for Plasma Research, University of Maryland, USA
Librarian, Fusion Energy Division, Oak Ridge National Laboratory, USA
Librarian, Institute of Fusion Studies, University of Texas, USA
Librarian, Magnetic Fusion Program, Lawrence Livermore National Laboratory, USA
Library, General Atomics, USA
Plasma Physics Group, Fusion Energy Research Program, University of California at San Diego, USA
Plasma Physics Library, Columbia University, USA
Alkesh Punjabi, Center for Fusion Research and Training, Hampton University, USA
Dr. W.M. Stacey, Fusion Research Center, Georgia Institute of Technology, USA
Director, Research Division, OFES, Washington, D.C. 20585-1290

The Princeton Plasma Physics Laboratory is operated
by Princeton University under contract
with the U.S. Department of Energy.

Information Services
Princeton Plasma Physics Laboratory
P.O. Box 451
Princeton, NJ 08543

Phone: 609-243-2750
Fax: 609-243-2751
e-mail: pppl_info@pppl.gov
Internet Address: http://www.pppl.gov